Giant Dielectric Response in the One-Dimensional Charge-Ordered Semiconductor $(NbSe_4)_3I$

D. Starešinić,[1,2] P. Lunkenheimer,[1] J. Hemberger,[1] K. Biljaković,[2] and A. Loidl[1]

[1]*Experimental Physics V, Center for Electronic Correlations and Magnetism, University of Augsburg, D-86135 Augsburg, Germany*

[2]*Institute of Physics, P.O. Box 304, HR-10001 Zagreb, Croatia*

(Received 13 June 2005; published 30 January 2006)

We report on broadband dielectric spectroscopy on the one-dimensional semiconductor $(NbSe_4)_3I$. Below the structural phase transition close to 270 K, which is accompanied by complex charge-order processes, we observe colossal dielectric constants with a frequency and temperature dependence very similar to what is observed in charge-density wave systems.

DOI: 10.1103/PhysRevLett.96.046402 PACS numbers: 71.45.Lr, 71.27.+a, 77.22.Gm

One-dimensional (1D) systems are fascinating topics of recent modern solid-state physics. More than 50 years ago, it was predicted by Peierls and Fröhlich that a one-dimensional electron gas coupled to phonons is unstable and undergoes a metal-to-insulator transition. Twenty years later, this new type of ground-state condensate, a charge-density wave (CDW), indeed was evidenced in highly anisotropic, approximately 1D materials. Iodine-doped transition-metal tetraselenides $(MSe_4)_nI$, with $M =$ Nb, Ta and $n = 2$, 3, and $10/3$, turned out to be paramount examples of materials with one-dimensional electronic structure [1–5]. For example, $(TaSe_4)_2I$, $(NbSe_4)_2I$, and $(NbSe_4)_{10/3}I$ are metallic at room temperature and undergo classical Peierls transitions with CDW formation at 263 [6,7], 220 [7], and 285 K [8], respectively. However, $(NbSe_4)_3I$ was found to be a charge-ordered semiconductor at room temperature, exhibiting a displacive structural phase transition at 274 K [9] to another insulating phase not associated with CDW formation. Recently, $(NbSe_4)_3I$ has been characterized by optical spectroscopy and photoemission as a quasi-1D insulator with unusual dynamic properties [10].

In the investigation of CDW systems, dielectric spectroscopy is a supreme technique. At audio frequencies, they reveal exceptionally large dielectric constants and strong dispersion effects as discussed in detail by Cava *et al.* [11,12] and as observed also for the systems $(TaSe_4)_2I$ and $(NbSe_4)_{10/3}I$ [13]. This was explained by Littlewood [14] in terms of screening effects on the randomly pinned CDW. Naively, the formation of CDWs can be viewed as a specific type of charge order (CO), although CO usually describes the localization of nonfractional charges. In transition-metal oxides, CO is a common phenomenon and an increasing number of dielectric measurements close to charge-ordering transitions are reported, specifically in low-dimensional systems, having in mind the close analogy to the Peierls transition in metallic systems. Indeed, a giant dielectric response has been detected in the insulating two-leg ladder $Sr_{14}Cu_{24}O_{41}$ [15,16], in the organic "Fabre salts" $(TMTTF)_2X$ (TMTTF denotes tetramethyltetrathiafulvalene) [17], and in one-dimensional $(DI\text{-}DCNQI)_2Ag$ (DCNQI denotes 2,5-diiodo-dicyanoquinonediimine) [18]. Thus, it seems promising to also investigate insulating charge-ordered tetraselenide $(NbSe_4)_3I$ by dielectric spectroscopy.

Single crystalline $(NbSe_4)_3I$ samples were grown by a conventional vapor transport technique and characterized by dc resistivity, heat capacity, and magnetization measurements [19]. From the heat capacity, we deduce a structural phase transition temperature of $T_c = 268 \pm 1$ K. The broadband dielectric response from 10 mHz to 100 MHz has been determined utilizing frequency-response analysis and a reflectometric technique [20]. Measurements on needle-shaped samples of cross section $\sim 1 \times 10^{-2}$ mm^2 and length 0.9–4.5 mm were performed along the crystallographic c direction for temperatures from 1.5 K $< T <$ 300 K. The typical amplitude of the driving signal of 0.1 V was well within the linear response regime. Special care has been taken to determine the true intrinsic dielectric response and to rule out contact or surface-layer contributions [21]. This has been done by performing measurements on samples with different contacts and with very different (up to a factor of 5) lengths.

Figure 1(a) shows the temperature dependence of the real part of the dielectric constant ε'. Starting at room temperature, ε' increases, reaches colossal values of the order of 10^5 between 100 and 200 K, and reveals a strong drop to values below 100 towards low temperatures. The inset in Fig. 1(a) shows the temperature-dependent static susceptibility obtained from an evaluation of the frequency-dependent data (cf. Fig. 2) for three samples with different thickness and contact material (silver paint and sputtered gold). From these and other detailed measurements with different contacts and sample geometries, we conclude that, while for $T > 200$ K contact contributions play a role, below 200 K all results represent the purely intrinsic dielectric response of $(NbSe_4)_3I$. Astonishingly, the temperature dependence of ε' closely resembles the observations in the CDW systems $(NbSe_4)_{10/3}I$ and $(TaSe_4)_2I$. In these compounds, the dielectric constant strongly increases in the Peierls state, reaching values of 10^6, and smoothly decreases towards

 © 2006 The American Physical Society

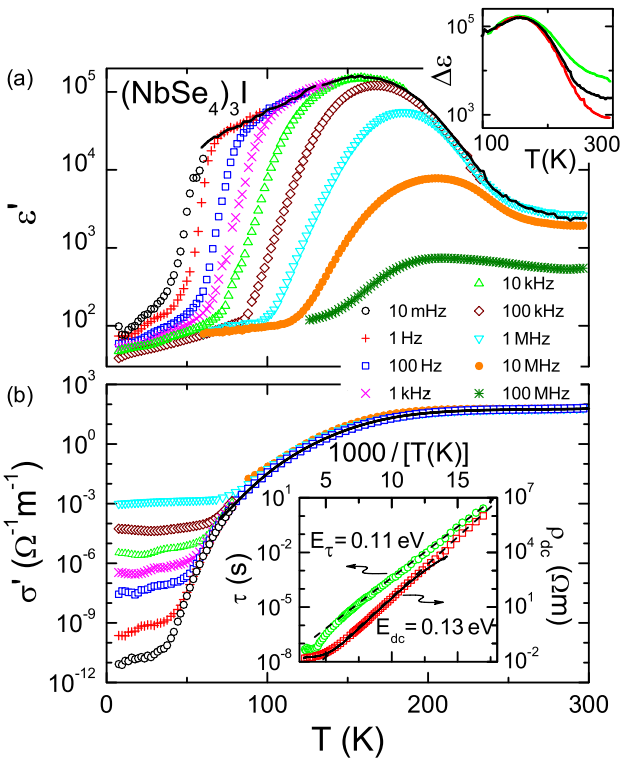

FIG. 1 (color online). (a) $\varepsilon'(\tau)$ and (b) $\sigma'(\tau)$ for various frequencies. The line in (a) represents the static susceptibility $\Delta\varepsilon$ as determined from an analysis of the data in Fig. 2. The upper inset shows $\Delta\varepsilon(\tau)$ obtained for three samples with different geometry and contact materials. The line in (b) is the dc conductivity measured by a standard 4-point technique. The lower inset shows the relaxation time (circles; from an analysis of the frequency-dependent spectra, Fig. 2) and the dc resistivity [solid line: 4-point measurement; squares: from $\sigma'(\nu)$] in an Arrhenius representation. The dashed lines demonstrate thermally activated behavior.

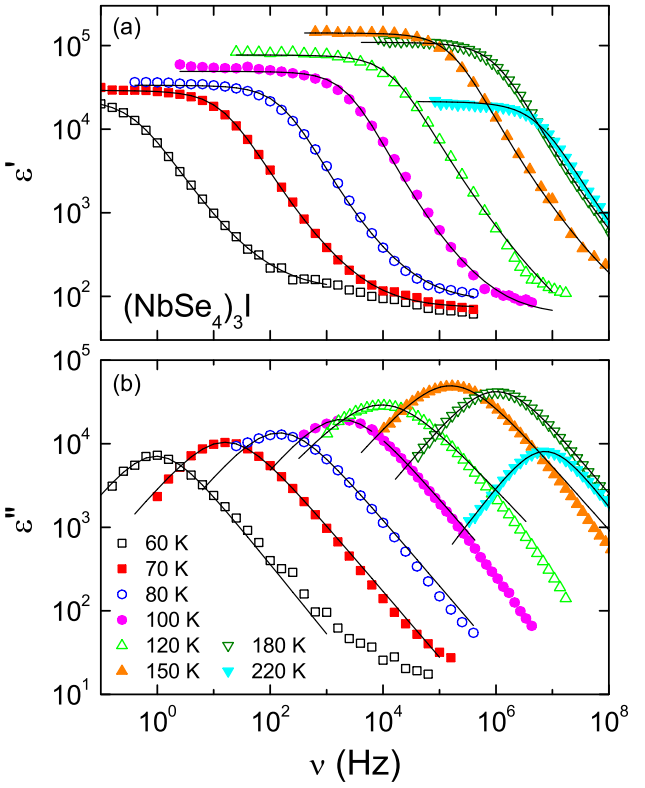

FIG. 2 (color online). (a) $\varepsilon'(\nu)$ and (b) $\varepsilon''(\nu)$ for various temperatures. The lines are fits with the empirical Cole-Cole function.

low temperatures, again revealing strong dispersion effects [13].

Figure 1(b) shows the conductivity $\sigma' = \omega\varepsilon_0\varepsilon''$, where $\omega = 2\pi\nu$, ε_0 is the permittivity of free space, and ε'' is the dielectric loss. Frequency-independent dc conductivity dominates for $T > 100$ K, while ac hopping conductivity comes into play at lower temperatures. The line indicates the result of a 4-point dc-conductivity measurement, performed down to 70 K. It precisely agrees with σ' measured at 10 mHz, giving further evidence that contact effects play no role. Also, the millimeter-wave results of Ref. [22], measured contact free utilizing quasioptic spectroscopy, are consistent with the temperature and frequency dependence shown in Fig. 1. In the inset in Fig. 1(b), the dc resistivity ρ_{dc} determined from the dielectric and the 4-point measurements is plotted in an Arrhenius representation (squares). The dashed line indicates that ρ_{dc} follows thermally activated behavior with a hindering barrier of 0.13 eV. The room-temperature resistivity of about 1.6 Ω cm is in good agreement with published results [9]. It is interesting that around room temperature the CDW-forming tetraselenides also exhibit a temperature dependence of the resistivity, which rather signals semiconducting behavior, regardless of the low absolute values of the order $1.5–3 \times 10^{-3}$ Ω cm in $(TaSe_4)_2I$ [6] and 1.5×10^{-2} Ω cm in $(NbSe_4)_{10/3}I$ [8].

Figure 2 documents the frequency dependence of (a) ε' and (b) ε'' for 60 K $< T <$ 220 K. The dielectric constant shows a steplike decrease on increasing frequency, which is typical for relaxational behavior. The point of inflection strongly shifts towards lower frequencies with decreasing temperature, indicating a slowing-down of the mean relaxation rate. To get an estimate of the relaxational part of the dielectric loss, the dc conductivity has been subtracted from the raw data, yielding well defined peaks, which also shift through the frequency window on decreasing temperature. $\varepsilon'(\nu)$ and $\varepsilon''(\nu)$ can be consistently described with the phenomenological Cole-Cole equation, which corresponds to symmetrically broadened Debye relaxation utilizing an extra width parameter α between 1 (Debye case) and 0 (infinitely broad). The broadening is commonly ascribed to a distribution of relaxation times. The results of the simultaneous fits to ε' and ε'' are indicated as lines in Fig. 2. The width parameter for all temperatures was close to 0.8, indicating a moderate distribution of relaxation times. The temperature dependence of the static dipolar susceptibility, determined by the height of the step of ε'

and by the area under the loss peaks, is indicated as solid line in Fig. 1(a). It closely follows the temperature dependence of ε' measured at 10 mHz down to 50 K. Finally, the temperature dependence of the mean relaxation time $\tau = 1/(2\pi\nu_p)$, with ν_p the maximum of the loss peaks, is shown in the inset in Fig. 1(b) (circles). Here we used an Arrhenius presentation, which leads to a linear dependence of τ between 60 and 150 K (dashed line), resulting in an energy barrier against thermal dipolar relaxations of 0.11 eV ($\approx$1300 K). This value is slightly lower than the barrier of 0.13 eV determined from $\rho_{dc}(T)$, which is plotted in the same frame.

The occurrence of a very strong relaxational mode in $(NbSe_4)_3I$ is unexpected and an interpretation not straight forward. To get an insight into this unusual behavior, one has to consider the crystalline structure of the tetraselenides: They crystallize in tetragonal structures with the transition metal arranged along the c axis separated by rectangular Se_4 units [schematically shown in Fig. 3(a)]. Two adjacent Se_4 rectangles are twisted by a well defined angle depending on the specific compound, and these MSe_4 chains are well separated by iodine ions. The Nb d_z^2 orbitals, which show overlap along c, are partly filled, e.g., with a filling of $1/4$ for $n = 2$ and $1/3$ for $n = 3$ and, hence, are expected to be metallic at high temperatures. This metallic phase is unstable against a Peierls distortion yielding a CDW state for $n = 2$ and $n = 10/3$. However, $(NbSe_4)_3I$ reveals a different ground state with a specific type of CO. This compound can be written as $Nb_2{}^{4+}Nb^{5+}(Se_2{}^{2-})_6I^-$ [5], and, hence, along the c axis a CO with a characteristic sequence of filled and empty d

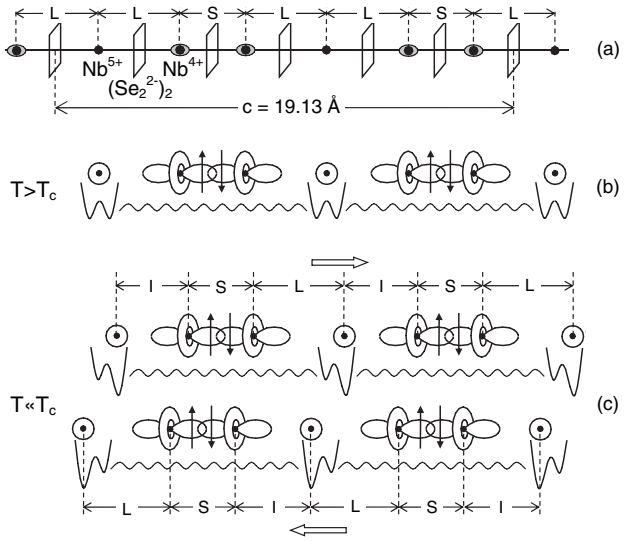

FIG. 3. Schematic drawing of the chain structure of $(NbSe_4)_3I$ above [(a) and (b)] and below (c) the structural phase transition temperature $T_c = 270$ K. In (a), the twist between adjacent Se_4 rectangles is omitted. In (b) and (c), only the Nb ions are shown. In the low-temperature phase, the two chains are shifted with respect to each other by approximately 0.4 Å. This is schematically indicated by the arrows.

orbitals, namely, $Nb^{4+}(d^1)$, $Nb^{4+}(d^1)$, and $Nb^{5+}(d^0)$, with concomitant orbital order is realized [Fig. 3(b)] [23]. There are strong covalent bonds between d^1 ions and weak bonds between d^1 and d^0 niobium ions. As there is a sequence of six differently oriented Se_4 rectangles per unit cell, the crystallographic structure consists of six Nb ions per chain and per lattice spacing. It exhibits a sequence of long (L: 0.325 nm) and short (S: 0.306 nm) Nb-Nb bond lengths, namely, $LLSLLS$, with the short bonds between the Nb^{4+} ions [Figs. 3(a) and 3(b)]. Obviously, the d^1 orbitals exhibit an orbital-derived dimerization with d_z^2-d_z^2 dimers characterized by a short bond length and by a spin singlet. These Nb^{4+} dimers are separated by single Nb^{5+} ions without any orbital and spin degrees of freedom. At the structural phase transition close to 270 K, the Nb^{5+} becomes attached closer to one dimer, and the sequence of bond lengths now becomes $LISLIS$, with an additional intermediate (I) bond length (I: 0.317 nm), a slightly increased bond L (0.331 nm), and S (0.306 nm) remaining almost unchanged [Fig. 3(c)] [5]. From this observation, it is clear that in the high-temperature phase the Nb^{5+} ion is located in a double-well potential, on cooling selecting one side as a stable equilibrium position. This situation corresponds to an order-disorder transition, strongly competing with thermal activation. In the absence of interaction, the Nb^{5+} ions would freeze-in randomly in one of the minima of the double-well potential. However, from structural investigations at low temperatures [5], we know that long-range order of the Nb^{5+} ions within the double well is established, which can be achieved via strong cooperative effects as indicated by the wavy lines in Figs. 3(b) and 3(c). Here the electric dipole-dipole coupling may play an important role. Only this cooperativity explains the occurrence of a ferrodistortive phase transition. At the same time, two neighboring $NbSe_4$ chains are shifted against each other [5], the overall situation being sketched in Fig. 3. Probably, this relative shift of the chains and the formation of asymmetric double-well potentials for the Nb^{5+} ions are highly correlated.

The structural phase transition, outlined above, seems to provide a natural explanation of the giant dielectric response in $(NbSe_4)_3I$. A comparison of the bond lengths of the low- and high-temperature phases allows an estimate of the dipole moment of Nb^{5+} in its double-well potential. The dipole moment d, defined as *charge* times *length*, results in $d = 5e \times 0.08$ Å $= 0.4e$ Å, corresponding to approximately 2 Debye. This dipole moment, while relatively large, however, cannot explain values of the dielectric constant reaching up to 10^5. The shift of the single chains against each other certainly plays an additional important role in establishing the colossal dielectric constants. We also would like to stress that, viewed from a single chain, the low-temperature phase should be ferroelectric, while there is antiferroelectric order between the chains. All Nb^{5+} ions are cooperatively attached closer to one Nb^{4+}, thus constituting ferroelectric order along one

chain [see Fig. 3(c)]. Indeed, the dielectric response of $(NbSe_4)_3I$ resembles that of relaxor ferroelectrics, namely, a Curie-Weiss–like increase of the dielectric permittivity, followed by a broad smeared out cusp and a subsequent fast decrease with considerable dispersion [24]. Usually, relaxor behavior is observed in diluted 3D ferroelectrics, where long-range polar order is suppressed by disorder and frustration. However, the tetraselenide under investigation is a pure, stoichiometric compound, and one might speculate that ferroelectricity is suppressed by the dimensionality, analogous to the absence of long-range magnetic order in 1D spin chains. It was only very recently that ferroelectricity has been reported in one-dimensional $(TMTTF)_2X$ ($X = PF_6$, AsF_6 and SbF_6) compounds [17], which reveal considerable dispersion close to T_c [25], and the high values of ε' in $(NbSe_4)_3I$ may arise from the high polarizability of the quasi-1D electron system coupled to atomic displacements, just as discussed in Ref. [17]. In $(NbSe_4)_3I$, one-dimensional ferroelectric correlations certainly play a role; however, according to present knowledge, the low-temperature structure of $(NbSe_4)_3I$ is noncentrosymmetric but with no polar axis [5], and, from a 3D point of view, ferroelectricity should not be expected. We also were not able to detect any pyrocurrents or ferroelectric hysteresis effects, which of course could result from relatively strong conductivity contributions.

Since the occurrence of polar order in $(NbSe_4)_3I$ cannot be finally proven, it may be essential to stress that the conductivity above and below T_c and the dielectric response below T_c in $(NbSe_4)_nI$, with $n = 3$, closely resemble the observations in the CDW systems with $n = 2$ and $n = 10/3$. However, structural details (see Fig. 3) indicate that the high-temperature phase reveals a specific charge order and at T_c only the charge distribution slightly changes. One may speculate that the low-temperature charge distribution may represent a specific type of CDW, with the same underlying characteristic fingerprints as observed in canonical CDW systems. In these systems, impurity pinning locks the sliding CDW into preferred positions. A pinning mode appears at high frequencies, and the low-frequency dielectric response results from screening effects of the pinned CDW by free charge carriers [14]. The existence of an inhomogeneously broadened relaxation mode with a time scale that follows the dc resistivity is in accord with our observations (inset in Fig. 1) and seems to favor a CDW interpretation. However, the physics behind this relaxation mechanism may not be specific to the CDW case, and the charge ordering of the Nb ions may be screened exactly the same way as a CDW. Above, we have described $(NbSe_4)_3I$ in a purely ionic picture with a specific charge order resulting in d^1-d^1-d^0 configurations of the niobium ions. It is unclear and has to be further investigated if a rather localized object such as this can move through the lattice via charge transfer along the chains. To prove or disprove the CDW interpretation, it seems essential to measure the depinning properties and to search for the pinning mode in the gigahertz range. Both types of experiments are presently under way.

In conclusion, dielectric spectroscopy on the charge-ordered 1D tetraselenide $(NbSe_4)_3I$ revealed an extremely strong relaxational mode and colossal intrinsic values of the dielectric constant. Considering the crystalline structure of this compound, an explanation in terms of correlated displacive ionic motions seems suggestive. However, having in mind the close resemblance to CDW systems, a CDW-like mechanism may also play a role, and further experiments are necessary to clarify this issue.

We thank Professor F. Levy for providing the samples. This work was supported by the Deutsche Forschungsgemeinschaft via the Sonderforschungsbereich 484 and by the BMBF via VDI/EKM. D. S. has been supported by the Alexander von Humboldt Foundation.

[1] A. Meerschaut, P. Palvadeau, and J. Rouxel, J. Solid State Chem. **20**, 21 (1977).
[2] J. Rouxel, Mol. Cryst. Liq. Cryst. **81**, 749 (1982).
[3] P. Gressier *et al.*, Inorg. Chem. **23**, 1221 (1984).
[4] C. Roucaut *et al.*, J. Phys. C **17**, 2993 (1984).
[5] P. Gressier, L. Guemas, and A. Meerschaut, Mater. Res. Bull. **20**, 539 (1985).
[6] Z. Z. Wang *et al.*, Solid State Commun. **46**, 325 (1983); M. Maki *et al.*, *ibid.* **46**, 497 (1983).
[7] H. Fujishita, M. Sato, and S. Hoshino, Solid State Commun. **49**, 313 (1984).
[8] Z. Z. Wang *et al.*, Solid State Commun. **47**, 439 (1983).
[9] M. Izumi *et al.*, Solid State Commun. **49**, 423 (1984); M. Izumi, T. Iwazumi, and K. Uchinokura, *ibid.* **51**, 191 (1984); T. Sekine *et al.*, *ibid.* **52**, 379 (1984).
[10] V. Vescoli *et al.*, Phys. Rev. Lett. **84**, 1272 (2000).
[11] R. J. Cava *et al.*, Phys. Rev. B **30**, 3228 (1984).
[12] R. J. Cava *et al.*, Phys. Rev. B **33**, 2439 (1986).
[13] T. Sekine, T. Tsuchiya, and E. Matsuura, Physica (Amsterdam) **143B+C**, 158 (1986).
[14] P. B. Littlewood, Phys. Rev. B **36**, 3108 (1987).
[15] B. Gorshunov *et al.*, Phys. Rev. B **66**, 060508(R) (2002).
[16] G. Blumberg *et al.*, Science **297**, 584 (2002).
[17] P. Monceau *et al.*, Phys. Rev. Lett. **86**, 4080 (2001).
[18] F. Nad *et al.*, J. Phys. Condens. Matter **16**, 7107 (2004).
[19] J. Hemberger *et al.* (to be published).
[20] P. Lunkenheimer *et al.*, Contemp. Phys. **41**, 15 (2000).
[21] P. Lunkenheimer *et al.*, Phys. Rev. B **66**, 052105 (2002); **70**, 172102 (2004).
[22] V. Zelezny *et al.*, J. Phys. Condens. Matter **1**, 10 585 (1989).
[23] However, it should be noted that a purely ionic picture may be oversimplified; see P. Gressier *et al.*, J. Solid State Chem. **51**, 141 (1984).
[24] L. E. Cross, Ferroelectrics **76**, 241 (1987).
[25] D. Starešinić *et al.*, Solid State Commun. **137**, 241 (2006).